JVI Journals.ASM.org

Palmitoylation on Conserved and Nonconserved Cysteines of Murine IFITM1 Regulates Its Stability and Anti-Influenza A Virus Activity

Jocelyn C. Hach, Temet McMichael, Nicholas M. Chesarino, Jacob S. Yount

Department of Microbial Infection and Immunity, Center for Microbial Interface Biology, The Ohio State University, Columbus, Ohio, USA

The interferon-induced transmembrane proteins (IFITMs) restrict infection by numerous viruses, yet the importance and regulation of individual isoforms remains unclear. Here, we report that murine IFITM1 (mIFITM1) is palmitoylated on one nonconserved cysteine and three conserved cysteines that are required for anti-influenza A virus activity. Additionally, palmitoylation of mIFITM1 regulates protein stability by preventing proteasomal degradation, and modification of the nonconserved cysteine at the mIFITM1 C terminus supports an intramembrane topology with mechanistic implications.

The interferon-induced transmembrane proteins (IFITMs) have been described to inhibit infection by a wide range of viruses, including important human pathogens such as influenza virus, West Nile virus, severe acute respiratory syndrome (SARS) coronavirus, human immunodeficiency virus, and dengue virus (1–6). The viruses that are restricted share the common ability to enter cells through endocytosis, and the restriction is indeed dependent upon the glycoproteins used for cellular entry (1, 2). Inhibition by IFITM3 occurs prior to influenza virus fusion with the endosome (7), which is a primary site of IFITM3 localization (2, 7, 8). IFITM3 appears to promote acidification or merging of endosomes with lysosomes, thereby exposing viral particles to a degradative environment (7–9). Consistent with this model, IFITM3 has recently been shown to reduce membrane fluidity and alter the curvature of membranes in such a way that virus hemifusion from within the endosome is inhibited while the fusion of opposing membranes possessing IFITMs may be enhanced (10).

The mechanism by which IFITMs change membrane curvature and the endolysosomal compartment is unknown. Addressing this question, we have recently proposed that the predicted dual transmembrane topology for IFITM3 is incorrect and that the active protein instead contains intramembrane domains that do not fully span the lipid bilayer (Fig. 1A and B) (8). Partial insertion of intramembrane domains into the membrane bilayer is well understood to promote curvature by virtue of the bilayer couple effect (Fig. 1B) (11). Evidence for this topology emerges largely from analysis of posttranslational modifications of IFITM3. Mass spectrometry and mutational analysis identified ubiquitination of lysine 24 (K24) on the IFITM3 N terminus (8). If the predicted topology is adopted, this residue would reside in the endoplasmic reticulum (ER) or endosomal lumen. However, known ubiquitin ligases are cytoplasmic, suggesting that the IFITM3 N terminus is localized in the cytoplasm. This is also supported by the discovery that phosphorylation of IFITM3 on tyrosine 20 (Y20) by the cytoplasmic kinase Fyn is required for IFITM3 antiviral activity (12). We further tested this alternative topology hypothesis by demonstrating that neither the N nor the C terminus nor the central loop domain of IFITM3 is exposed to the ER lumen glycosylation machinery but an antivirally active IFITM3 mutant engineered to possess myristoylation and prenylation motifs can be modified at its N terminus and C terminus by cytoplasmic myristoylation and prenylation enzymes, respectively (8). Moreover, our discovery of IFITM3 palmitoylation, a 16-carbon lipid modification, occurring on cysteine 71 (C71), C72, and C105 within or adjacent to the two hydrophobic domains (3) is consistent with an intramembrane topology, as palmitoylation is a typical feature of known intramembrane proteins (13, 14), indicating that this modification may be involved in recruiting or anchoring intramembrane domains to membranes.

Thus, there is strong evidence that the N terminus of human and mouse IFITM3 is cytoplasmic, and yet, the topology of active IFITMs remains controversial due to earlier immunostaining experiments indicating that both the N and C termini of IFITM3 are extracellular (1, 15). We hypothesized that murine IFITM1 (mIFITM1), which possesses strong homology to mIFITM3 (74 of 106 amino acids are identical to those in mIFITM3) (Fig. 1C) and has not been analyzed regarding posttranslational modifications, may serendipitously provide evidence that the C terminus of a naturally occurring and antivirally active IFITM variant is exposed to cytoplasmic enzymes. mIFITM1 possesses three conserved cysteines (C49, C50, and C83) that are known to be palmitoylated on IFITM3 and necessary for its complete anti-influenza virus activity (3), but it also contains a fourth, nonconserved cysteine near its C terminus (C103) that is not found in most other IFITMs, including the homologous human IFITM1. We cloned mIFITM1 into the pCMV-HA vector (Clontech) and made single cysteine mutants in order to examine the contribution of each of these cysteines to mIFITM1 palmitoylation. To measure palmitoylation, HEK293T cells in 6-well plates were transfected overnight with 1.0 μg of wild-type (WT) hemagglutinin-conjugated mIFITM1 (HA-mIFITM1) or cysteine-to-alanine mutants using Lipofectamine 2000 (Life Technologies). Cells were then metabolically labeled for 1 h with the alk-16 chemical reporter of protein palmitoylation (kindly provided by Howard C. Hang, Rockefeller University) (16, 17) or dimethyl sulfoxide (DMSO) as a control. Lysates were subjected to immunoprecipitation with anti-HA-agarose antibody (Sigma). Precipitated protein was reacted with azido-rhodamine (az-rho) via the copper-catalyzed azide-alkyne

Received 5 March 2013 **Accepted** 17 June 2013
Published ahead of print 26 June 2013
Address correspondence to Jacob S. Yount, yount.37@osu.edu.

doi:10.1128/JVI.00621-13

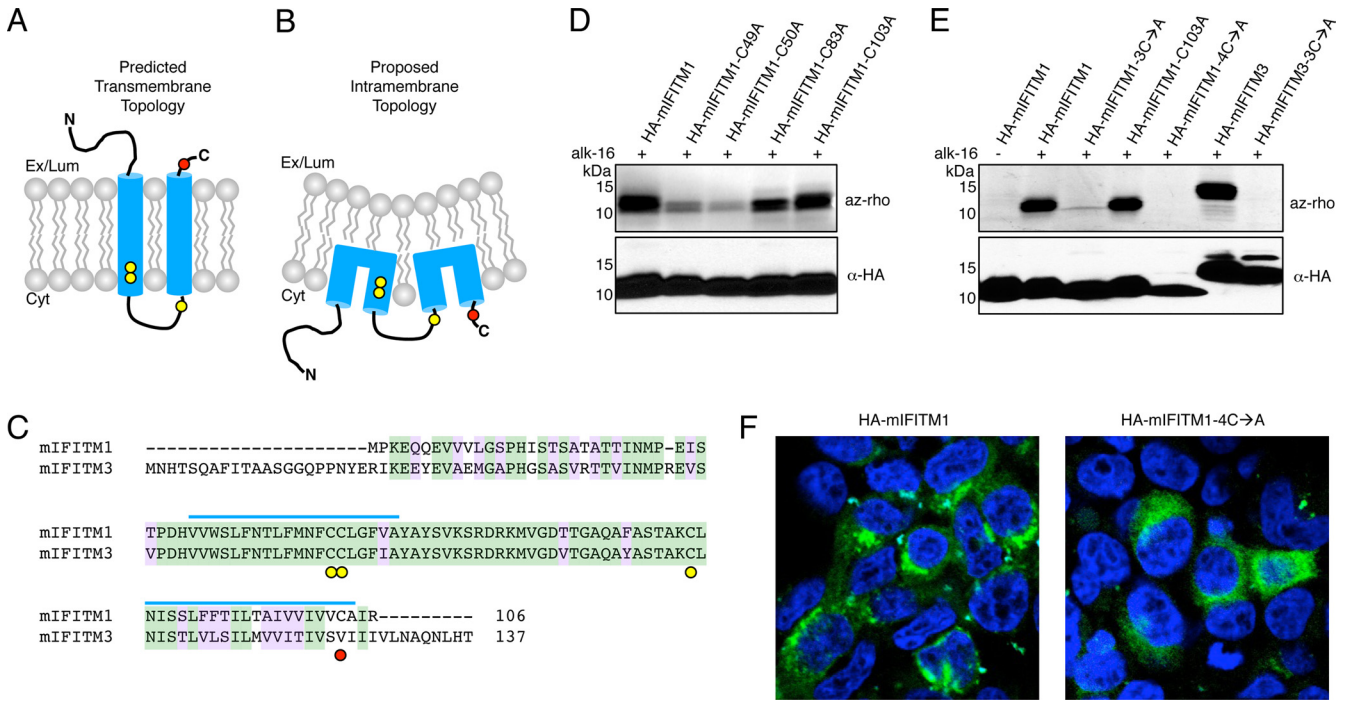

FIG 1 mIFITM1 is palmitoylated on conserved and nonconserved cysteines. (A, B) Potential transmembrane or intramembrane protein topologies for IFITMs are depicted. Yellow circles indicate approximate locations of conserved cysteines, and the red circle indicates the approximate location of the nonconserved cysteine at position 103 in mIFITM1. (C) Alignment of mIFITM1 and mIFITM3 is shown. Green shading indicates identical residues, and purple shading indicates conservative amino acid substitutions based on the Gonnet PAM 250 matrix (28). Blue lines indicate hydrophobic domains, and yellow and red circles indicate positions of conserved and nonconserved cysteines, respectively. (D to F) HEK293T cells were transfected overnight in 6-well plates with 1 μg/well of plasmids expressing HA-mIFITM1, HA-IFITM1-C49A, HA-IFITM1-C50A, HA-IFITM1-C83A, HA-mIFITM-C103A, or HA-mIFITM3 or with 4 μg/well of plasmids expressing HA-mIFITM1-3C→A or HA-mIFITM1-4C→A. Total amounts of DNA transfected in the experiment whose results are shown in panel E were equalized using empty vector. For the experiments whose results are shown in panels D and E, 1 h of labeling with 50 μM alk-16 or DMSO as a control was performed, and 1.5 mg protein in lysates was subjected to immunoprecipitation with anti-HA-agarose antibody and reacted by click chemistry with azido-rhodamine (az-rho) prior to fluorescence gel scanning to visualize levels of protein palmitoylation. Western blotting with anti-HA antibody demonstrated comparable protein loading. Data are representative of three experiments. For the experiment whose results are shown in panel F, cells were visualized by confocal microscopy after paraformaldehyde fixation and staining with anti-HA antibody (green) and 4′,6′-diamidino-2-phenylindole (DAPI; blue).

cycloaddition reaction commonly termed "click chemistry" to tag alk-16-labeled proteins prior to SDS-PAGE (3, 16, 17). Fluorescence gel scanning allowed visualization of palmitoylation, and immunoblotting (anti-HA antibody; Clontech) was performed to show comparable protein loading (Fig. 1D). The results of this study clearly indicated that each of the mIFITM1 conserved cysteines contributed to mIFITM1 palmitoylation but that loss of C103 did not dramatically decrease palmitoylation in the presence of the intact conserved cysteines.

We next generated mIFITM1 mutants in which the three conserved cysteines were mutated to alanine (3C→A) or all four cysteines were mutated (4C→A) to test whether modification of C103 could be observed in the absence of the conserved cysteines. The initial experiments with these constructs and previously described HA-mIFITM3 and HA-mIFITM3-3C→A (having C71, C72, and C105 mutated to A) constructs (3) indicated that the mIFITM1-3C→A and -4C→A mutants had uniquely poor expression but that this difficulty could be overcome by transfecting higher quantities of plasmid DNA for these mutants. An amount of 1.0 μg of the wild-type HA-mIFITM1, HA-mIFITM1-C103A, HA-mIFITM3, or HA-mIFITM3-3C→A construct or 4.0 μg of the HA-mIFITM1-3C→A or -4C→A mutant was transfected into HEK293T cells, and palmitoylation analysis was performed using the alk-16 chemical reporter and fluorescence gel scanning (Fig. 1E). These results demonstrate that mIFITM1 is primarily palmitoylated on its conserved three cysteines, similarly to IFITM3, but that palmitoylation can also occur on C103. Palmitoylation at the mIFITM1 C terminus would preclude adoption of the predicted topology and further supports an intramembrane topology model (Fig. 1B).

Given that palmitoylation of IFITM3 has been demonstrated to affect its localization, including its membrane affinity and homotypic clustering (3, 8, 18), we compared the cellular distribution of HA-mIFITM1 and the palmitoylation-deficient mIFITM1-4C→A by confocal microscopy. HA-mIFITM1 was observed to be primarily clustered in perinuclear compartments with some additional diffuse staining, while HA-mIFITM1-4C→A appeared mostly diffuse with minimal clustering (Fig. 1F). This imaging would suggest that palmitoylation plays a conserved role on the IFITMs in controlling their localization.

Having identified palmitoylation on the conserved and nonconserved cysteines of mIFITM1, we next examined the mechanism leading to poor expression of the 3C→A and 4C→A mutants, as we have repeatedly observed little effect of palmitoylation on the stability of mIFITM3 (Fig. 1C) (3, 8, 19). To test for proteasomal degradation of palmitoylation-deficient mIFITM1 mutants, we transfected cells with equal amounts of plasmids expressing HA-mIFITM1 or mutants. After overnight transfection, cells

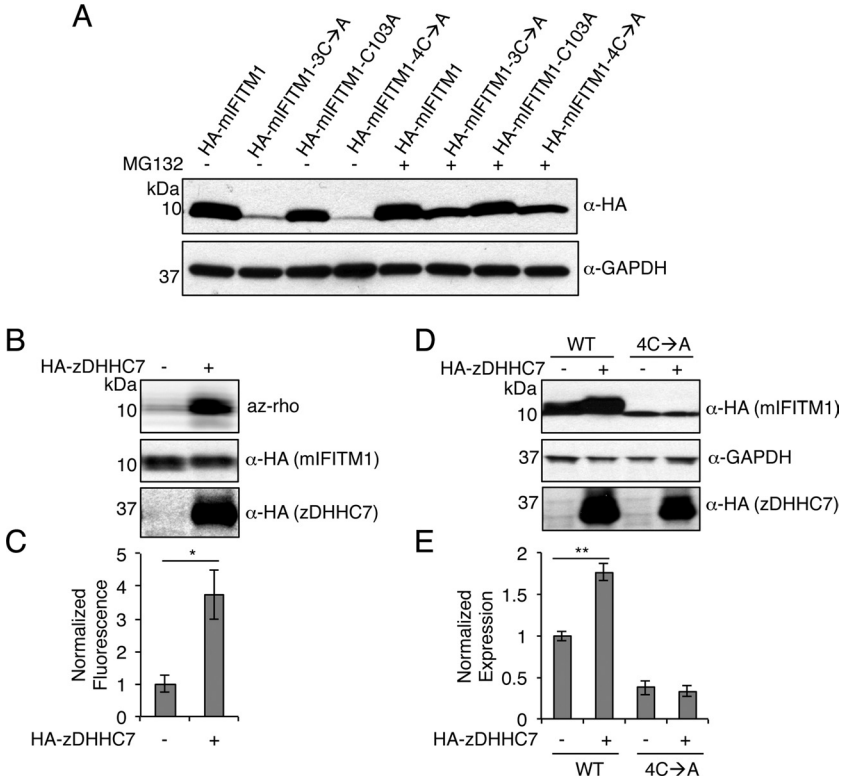

FIG 2 Palmitoylation of mIFITM1 prevents proteasomal degradation. (A) HEK293T cells were transfected overnight in 6-well plates with 1 μg/well plasmids expressing the indicated proteins. Cells were then treated for 24 h with 25 μM MG132 or DMSO as a control. Western blotting was performed with anti-HA antibodies to examine HA-mIFITM1 protein levels in the cells, and anti-glyceraldehyde-3-phosphate dehydrogenase (GAPDH) antibody was used to demonstrate comparable loading. Data are representative of three experiments. (B to E) Cells were transfected with 2 μg/well of plasmid expressing HA-mIFITM1 or HA-mIFITM1-4C→A in combination with 2 μg/well of plasmid expressing either GST or HA-zDHHC7. (B) An amount of 250 μg GST sample or 125 μg HA-zDHHC7 sample was subjected to immunoprecipitation with anti-HA-agarose antibody and reacted by click chemistry with azido-rhodamine (az-rho) prior to fluorescence gel scanning to visualize levels of protein palmitoylation. Western blotting with anti-HA antibody detected the amounts of HA-zDHHC7 and HA-mIFITM1 in the immunoprecipitates. (C) Quantification of palmitoylation signal from four experiments normalized for protein loading. Palmitoylation of HA-mIFITM1 in the presence of GST was set at a value of 1.0, and the error bars indicate the standard errors of the means of the four experiments. *, $P = 0.014$ by Student's *t* test. (D) Western blotting of cell lysates with anti-HA antibody demonstrated the levels of HA-mIFITM1, as well as the expression of HA-zDHHC7. Blotting with anti-GAPDH antibody provided a loading control. (E) Quantification of HA-mIFITM1 protein levels from six experiments and HA-mIFITM1-4C→A protein levels from three experiments normalized for protein loading. The level of HA-mIFITM1 in the presence of GST was set at a value of 1.0, and the error bars indicate the standard errors of the means. **, $P < 0.001$ by Student's *t* test.

were treated with 25 μM proteasome inhibitor MG132 (Sigma) or DMSO as a control for 24 h. Cell lysates were then separated by SDS-PAGE and probed for HA-mIFITM1 expression by immunoblotting. The poor expression observed for the 3C→A and 4C→A mutants was efficiently rescued by MG132 treatment (Fig. 2A), suggesting that palmitoylation serves to stabilize mIFITM1 by preventing proteasomal degradation. To further confirm this finding, we examined whether increasing mIFITM1 palmitoylation would promote higher cellular levels of this protein. Palmitoylation is installed onto proteins primarily by a family of enzymes known as the zinc finger Asp-His-His-Cys (zDHHC) domain-containing palmitoyltransferases (20, 21). zDHHC7 is among the most promiscuous of the mammalian zDHHC proteins in terms of substrate specificity (22), and we have found overexpression of this protein to be a useful tool to increase palmitoylation of multiple proteins. As such, the overexpression of HA-zDHHC7, compared to the overexpression of glutathione *S*-transferase (GST) as a control (both kindly provided by Masaki Fukata, National Institute for Physical Sciences, Japan) (23), significantly increased the palmitoylation of HA-mIFITM1, by approximately 4-fold (Fig. 2B and C). A corresponding 1.8-fold increase in the HA-mIFITM1 protein level was observed in cell lysates, while no change in the level of HA-mIFITM1-4C→A was observed upon zDHHC7 overexpression (Fig. 2D and E). The difference in fold changes observed for palmitoylation and overall protein level is likely due to palmitoylation occurring on multiple cysteines per mIFITM1 molecule. Overall, the examination of mIFITM1 has uncovered a previously undescribed role for palmitoylation of IFITMs in regulating protein stability and abundance.

To investigate the effect of palmitoylation of mIFITM1 on its anti-influenza virus activity, we sought to decouple the role of palmitoylation in regulating protein levels from a potential additional role in virus restriction. We achieved comparable expression levels of HA-mIFITM1 and its mutants as measured by flow cytometry by transfecting four times more plasmid DNA for the mIFITM1-3C→A and -4C→A mutants (Fig. 3A). The total amounts of DNA transfected were equalized using the empty pCMV-HA vector. The majority of HA-positive cells expressed comparable levels of protein, though cells transfected with palmitoylation-deficient mutants showed fewer cells expressing ex-

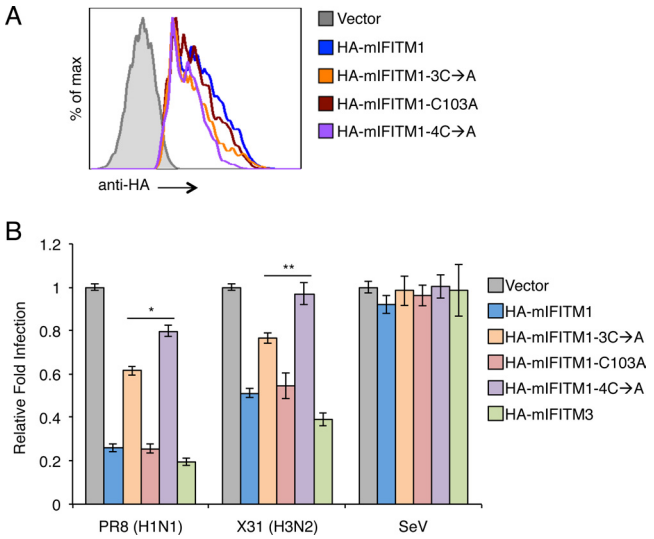

FIG 3 Palmitoylation on conserved and nonconserved cysteines of mIFITM1 is required for anti-influenza virus activity. (A, B) HEK293T cells were transfected overnight in 12-well plates with 0.5 μg/well of pCMV-HA as a vector control or plasmids expressing HA-mIFITM1, HA-mIFITM1C103A, or HA-mIFITM3 or with 2 μg/well of plasmids expressing HA-mIFITM1-3C→A or HA-mIFITM1-4C→A. Total amounts of DNA transfected were equalized using empty vector. Cells were then mock infected or infected with influenza A virus strain PR8 or X31 or Sendai virus (SeV) strain Cantell for 6 h at a multiplicity of infection of 2.5. Cells were fixed and stained with anti-HA antibodies to measure HA-mIFITM1 or -3 levels and with anti-influenza nucleoprotein antibody or anti-SeV polyclonal antiserum to identify infected cells. (A) HA-positive cells were gated based on lack of staining in the vector control and analyzed in histogram form to confirm comparable expression of HA-mIFITM1 and mutants. (B) HA-positive cells were gated as described for panel A and analyzed for percent infection based on anti-influenza nucleoprotein antibody or anti-SeV antiserum staining using noninfected samples as a baseline for gating. The average percent infection for vector control cells was set at 1.0 for each infection. The average values of at least six samples from at least two independent experiments were plotted for each virus, and error bars indicate standard errors of the means. *, $P = 0.004$, and **, $P = 0.02$, by Student's *t* test.

tremely high levels of the proteins (Fig. 3A). Transfected cells were mock infected or infected with influenza virus strain A/Puerto Rico/8/34 (H1N1) (PR8) at a multiplicity of infection of 2.5 for 6 h, fixed, and stained with anti-HA antibody (Covance) to identify cells expressing IFITMs. Cells were gated based on the expression of the IFITMs, and these subsets were analyzed for the percentage of cells that were infected as judged by positive staining with anti-influenza virus nucleoprotein antibodies (ab20343; Abcam). An empty vector transfection control provided a baseline for maximal infection (Fig. 3B). Cells expressing either HA-mIFITM1 or HA-mIFITM3 were significantly protected from infection, demonstrating that, when overexpressed, both of these proteins are similarly able to restrict influenza A virus infection (Fig. 3B). Mutation of the three conserved cysteines (3C→A) in HA-mIFITM1 resulted in an increased rate of infection compared to the results for WT HA-mIFITM1, though this protein still retained the ability to provide a reduction in infection compared to the results for vector control cells (Fig. 3B). The HA-mIFITM1-C103 mutant showed a similar ability to inhibit virus infection compared to the inhibition by HA-mIFITM1, though a role for C103 in contributing to antiviral activity was revealed when the conserved cysteines were also mutated (Fig. 3B, HA-mIFITM1-4C→A). Similar results were obtained when infecting with a second strain of influenza virus known as X31 (kindly provided by Thomas Moran and Bruno Moltedo, Mt. Sinai School of Medicine, New York, NY) (Fig. 3B). This virus is a reassortant of the PR8 virus containing the hemagglutinin and neuraminidase of influenza virus A/Aichi/2/1968, making X31 an H3N2 strain. We also performed a specificity control using Sendai virus (SeV) strain Cantell (ATCC). This prototypical paramyxovirus is well characterized to utilize pH-independent fusion at the cell surface (24) and would be expected to avoid IFITM restriction in the endolysosomal compartment. Indeed, no effect of IFITM1, IFITM1 mutants, or IFITM3 on the infection of HEK293T cells by this virus as analyzed using anti-SeV antibodies (code no. PD029; MBL) was observed by flow cytometry (Fig. 3B).

Overall, these data indicate that palmitoylation at C103 is largely redundant and can only partially compensate for loss of palmitoylation on the mIFITM1 conserved cysteines. Nonetheless, the clearly observed and reproducible change in antiviral activity between the mIFITM1-3C→A and -4C→A mutants demonstrates that modification of a naturally occurring and antivirally active IFITM variant at its C terminus by palmitoylation machinery known to exist in the cytoplasm contributes to anti-influenza virus activity, increasing the support for an intramembrane topology with both N and C termini facing the cytoplasm. This additional evidence for an IFITM intramembrane topology suggests that changes in membrane curvature upon IFITM expression may be driven directly by their partial bilayer insertion and the bilayer couple effect (Fig. 1B) (11). It will be interesting to determine whether IFITMs artificially targeted to other cellular organelles can exert an effect similar to their alteration of endosomes.

Two recent studies have demonstrated the essentiality of IFITM3 in protecting mouse models from influenza virus infections (25, 26). Interestingly, the progression of infection in mice missing all IFITMs was indistinguishable from the progression of infection by the knockout of IFITM3 alone (25, 26). It was also shown that a mutation in humans rendering IFITM3 inactive occurred more frequently in patients hospitalized for severe influenza virus infection than in a control population (25). These data suggest that IFITM1, though able to inhibit influenza virus in overexpression systems and despite expression in bronchial epithelium (27), is not able to compensate for the loss of IFITM3 *in vivo* (25, 26). This conundrum may be explained by the inherent instability of IFITM1, which requires palmitoylation to prevent its proteasomal degradation (Fig. 2). This is in contrast to IFITM3, which is robustly expressed even in the absence of palmitoylation (Fig. 1E) (3, 8, 19), perhaps allowing the time needed for palmitoylation and, thus, its maximal activation to occur. Our results demonstrate that increasing the palmitoylation levels of IFITM1 enhances its stability and could be of preventative or therapeutic benefit in the treatment of influenza virus disease, particularly in the absence of IFITM3.

ACKNOWLEDGMENTS

This work was supported by funding from the NIH/NIAID (grant AI095348 to J.S.Y.) and The Ohio State University. N.M.C. is supported by The Ohio State University Systems and Integrative Biology Training Program.

We thank Li Wu and Corine St. Gelais (The Ohio State University) for helpful suggestions and Howard Hang (Rockefeller University) for the kind gift of alk-16 and click chemistry reagents, Masaki Fukata (NIPS,

Japan) for providing zDHHC7 and GST constructs, and Thomas Moran and Bruno Moltedo (Mt. Sinai School of Medicine) for providing the X31 influenza virus strain.

REFERENCES

1. **Brass AL, Huang IC, Benita Y, John SP, Krishnan MN, Feeley EM, Ryan BJ, Weyer JL, van der Weyden L, Fikrig E, Adams DJ, Xavier RJ, Farzan M, Elledge SJ.** 2009. The IFITM proteins mediate cellular resistance to influenza A H1N1 virus, West Nile virus, and dengue virus. Cell **139:**1243–1254.
2. **Huang IC, Bailey CC, Weyer JL, Radoshitzky SR, Becker MM, Chiang JJ, Brass AL, Ahmed AA, Chi X, Dong L, Longobardi LE, Boltz D, Kuhn JH, Elledge SJ, Bavari S, Denison MR, Choe H, Farzan M.** 2011. Distinct patterns of IFITM-mediated restriction of filoviruses, SARS coronavirus, and influenza A virus. PLoS Pathog. **7:**e1001258. doi:10.1371/journal.ppat.1001258.
3. **Yount JS, Moltedo B, Yang YY, Charron G, Moran TM, Lopez CB, Hang HC.** 2010. Palmitoylome profiling reveals S-palmitoylation-dependent antiviral activity of IFITM3. Nat. Chem. Biol. **6:**610–614.
4. **Lu J, Pan Q, Rong L, He W, Liu SL, Liang C.** 2011. The IFITM proteins inhibit HIV-1 infection. J. Virol. **85:**2126–2137.
5. **Weidner JM, Jiang D, Pan XB, Chang J, Block TM, Guo JT.** 2010. Interferon-induced cell membrane proteins, IFITM3 and tetherin, inhibit vesicular stomatitis virus infection via distinct mechanisms. J. Virol. **84:**12646–12657.
6. **Schoggins JW, Wilson SJ, Panis M, Murphy MY, Jones CT, Bieniasz P, Rice CM.** 2011. A diverse range of gene products are effectors of the type I interferon antiviral response. Nature **472:**481–485.
7. **Feeley EM, Sims JS, John SP, Chin CR, Pertel T, Chen LM, Gaiha GD, Ryan BJ, Donis RO, Elledge SJ, Brass AL.** 2011. IFITM3 inhibits influenza A virus infection by preventing cytosolic entry. PLoS Pathog. **7:**e1002337. doi:10.1371/journal.ppat.1002337.
8. **Yount JS, Karssemeijer RA, Hang HC.** 2012. S-palmitoylation and ubiquitination differentially regulate interferon-induced transmembrane protein 3 (IFITM3)-mediated resistance to influenza virus. J. Biol. Chem. **287:**19631–19641.
9. **Wee YS, Roundy KM, Weis JJ, Weis JH.** 2012. Interferon-inducible transmembrane proteins of the innate immune response act as membrane organizers by influencing clathrin and v-ATPase localization and function. Innate Immun. **18:**834–845.
10. **Li K, Markosyan RM, Zheng YM, Golfetto O, Bungart B, Li M, Ding S, He Y, Liang C, Lee JC, Gratton E, Cohen FS, Liu SL.** 2013. IFITM proteins restrict viral membrane hemifusion. PLoS Pathog. **9:**e1003124. doi:10.1371/journal.ppat.1003124.
11. **Voeltz GK, Prinz WA.** 2007. Sheets, ribbons and tubules—how organelles get their shape. Nat. Rev. Mol. Cell Biol. **8:**258–264.
12. **Jia R, Pan Q, Ding S, Rong L, Liu SL, Geng Y, Qiao W, Liang C.** 2012. The N-terminal region of IFITM3 modulates its antiviral activity by regulating IFITM3 cellular localization. J. Virol. **86:**13697–13707.
13. **Dietzen DJ, Hastings WR, Lublin DM.** 1995. Caveolin is palmitoylated on multiple cysteine residues. Palmitoylation is not necessary for localization of caveolin to caveolae. J. Biol. Chem. **270:**6838–6842.
14. **Snyers L, Umlauf E, Prohaska R.** 1999. Cysteine 29 is the major palmitoylation site on stomatin. FEBS Lett. **449:**101–104.
15. **Diamond MS, Farzan M.** 2013. The broad-spectrum antiviral functions of IFIT and IFITM proteins. Nat. Rev. Immunol. **13:**46–57.
16. **Charron G, Zhang MM, Yount JS, Wilson J, Raghavan AS, Shamir E, Hang HC.** 2009. Robust fluorescent detection of protein fatty-acylation with chemical reporters. J. Am. Chem. Soc. **131:**4967–4975.
17. **Yount JS, Zhang MM, Hang HC.** 2011. Visualization and identification of fatty acylated proteins using chemical reporters. Curr. Protoc. Chem. Biol. **3:**65–79.
18. **Chutiwitoonchai N, Hiyoshi M, Hiyoshi-Yoshidomi Y, Hashimoto M, Tokunaga K, Suzu S.** 2013. Characteristics of IFITM, the newly identified IFN-inducible anti-HIV-1 family proteins. Microbes Infect. **15:**280–290.
19. **Yount JS, Charron G, Hang HC.** 2012. Bioorthogonal proteomics of 15-hexadecynyloxyacetic acid chemical reporter reveals preferential targeting of fatty acid modified proteins and biosynthetic enzymes. Bioorg. Med. Chem. **20:**650–654.
20. **Mitchell DA, Vasudevan A, Linder ME, Deschenes RJ.** 2006. Protein palmitoylation by a family of DHHC protein S-acyltransferases. J. Lipid Res. **47:**1118–1127.
21. **Linder ME, Jennings BC.** 2013. Mechanism and function of DHHC S-acyltransferases. Biochem. Soc. Trans. **41:**29–34.
22. **Greaves J, Chamberlain LH.** 2011. DHHC palmitoyl transferases: substrate interactions and (patho)physiology. Trends Biochem. Sci. **36:**245–253.
23. **Fukata M, Fukata Y, Adesnik H, Nicoll RA, Bredt DS.** 2004. Identification of PSD-95 palmitoylating enzymes. Neuron **44:**987–996.
24. **Hoekstra D, Klappe K, de Boer T, Wilschut J.** 1985. Characterization of the fusogenic properties of Sendai virus: kinetics of fusion with erythrocyte membranes. Biochemistry **24:**4739–4745.
25. **Everitt AR, Clare S, Pertel T, John SP, Wash RS, Smith SE, Chin CR, Feeley EM, Sims JS, Adams DJ, Wise HM, Kane L, Goulding D, Digard P, Anttila V, Baillie JK, Walsh TS, Hume DA, Palotie A, Xue Y, Colonna V, Tyler-Smith C, Dunning J, Gordon SB, Smyth RL, Openshaw PJ, Dougan G, Brass AL, Kellam P.** 2012. IFITM3 restricts the morbidity and mortality associated with influenza. Nature **484:**519–523.
26. **Bailey CC, Huang IC, Kam C, Farzan M.** 2012. Ifitm3 limits the severity of acute influenza in mice. PLoS Pathog. **8:**e1002909. doi:10.1371/journal.ppat.1002909.
27. **Klymiuk I, Kenner L, Adler T, Busch DH, Boersma A, Irmler M, Fridrich B, Gailus-Durner V, Fuchs H, Leitner N, Muller M, Kuhn R, Schlederer M, Treise I, de Angelis MH, Beckers J.** 2012. In vivo functional requirement of the mouse Ifitm1 gene for germ cell development, interferon mediated immune response and somitogenesis. PLoS One **7:**e44609. doi:10.1371/journal.pone.0044609.
28. **Benner SA, Cohen MA, Gonnet GH.** 1994. Amino acid substitution during functionally constrained divergent evolution of protein sequences. Protein Eng. **7:**1323–1332.